JOURNAL OF CATALYSIS 84, 156–169 (1983)

Multiple Isotope Tracing of Methanation over Nickel Catalyst

III. Completion of ^{13}C and D Tracing

M. OTAROD, S. OZAWA,[1] F. YIN,[2] M. CHEW, H. Y. CHEH, AND J. HAPPEL[3]

Department of Chemical Engineering and Applied Chemistry, Columbia University, New York, New York 10027

Received March 14, 1983; revised June 14, 1983

The methanation of mixtures of carbon monoxide and hydrogen was studied by a transient superposition technique using terminal species marked by ^{13}C and D. Further evidence is presented that the most abundant reacting intermediate is the species CH_{ads}. It appears that the hydrogenation of this species controls the rate of methanation. Carbidic carbon consists of relatively small pool of active C_{ads} together with a larger pool of carbon which, although not active for methanation, is also not graphitic. A mechanism is presented which summarizes the findings of this and the previous two papers in this series.

INTRODUCTION

This study in this series is preceded by two papers in which the mechanism of methanation was modeled based on transient isotope tracing. In the first paper (Happel *et al.* (*1*)) conducted experiments using ^{13}C, ^{18}O, and D as tracers. Their study showed that hydrogenation of $CH_{x,ads}$ intermediates was an important factor in the mechanism, based mostly on ^{13}C tracing data. A second paper, (Happel *et al.* (*2*)) concentrated on the modeling of data obtained by the transient appearance of deuteromethanes by D tracing. It confirmed the findings of Part I and identified the CH_{ads} species as being more abundant than either $CH_{2,ads}$ or $CH_{3,ads}$.

In Part II the results obtained by titration of the surface species using deuterium indicated the presence of more carbidic carbon than was accounted for by ^{13}C in the study in Part I. This would indicate that the surface concentration of reactive carbon entering into the mechanism is relatively small. Studies by Biloen *et al.* (*3*) using transient tracing employing ^{13}C also showed that only a small proportion of the carbidic layer that develops in methanation and the Fischer–Tropsch synthesis employing nickel, cobalt, and ruthenium catalysts belongs to reaction intermediates.

Happel *et al.* (*4*) in ^{13}C tracing studies reported after the study in Part I concluded that under methanation conditions carbon in carbon monoxide does not exchange readily with chemisorbed carbidic carbon (as had been originally assumed in Part I). Thus the step in which chemisorbed CO dissociates to produce carbidic carbon was then taken as unidirectional, as is also the case in the present study. This is in agreement with particularly relevant studies by Biloen *et al.* (*5*) in which catalysts were precovered with labeled surface carbon and then subjected to CO/H_2 mixtures. It was found by Biloen and also Araki and Ponec (*6*) that labeled carbon was transferred to produce CH_4 rather than to unconverted feed CO, although exchange with undissociated CO is close to equilibrium. This is

[1] Present address: Department of Chemical Engineering, Tohoku University, Aobo Aramaki, Sendai, Japan 980.

[2] Present address: Institute of Daily Chemical Industry, Ministry of Light Industry, Taiyuan, People's Republic of China.

[3] To whom all correspondence should be addressed.

0021-9517/83 $3.00
Copyright © 1983 by Academic Press, Inc.
All rights of reproduction in any form reserved.

indicative of a sequence in which oxygen in CO is being removed as CO_2 or as H_2O, in an essentially unidirectional step.

Another indication of the fast rate of methanation relative to recombination of surface carbon and oxygen atoms is given by studies of isotopic scrambling of $^{13}C^{16}O$ and $^{12}C^{18}O$ by Cant and Bell (*7*). In these studies conducted during simultaneous methanation over a ruthenium–silica catalyst, less than 1 molecule in 40 of oxygen underwent mixing relative to methanation. When the flow of hydrogen to the system was shut off, the scrambling increased somewhat but was still much slower than the methanation rate. These authors also presented data confirming the very rapid exchange of chemisorbed CO with gas phase CO.

In this paper ^{13}C studies are reported which are aimed at obtaining more quantitative information on the extent of surface coverage by inactive carbidic carbon as well as elucidating the mechanism of transfer of carbon to CO_2 more exactly. Data are also presented for deuterium tracing to water.

Finally, the results of these studies are combined to indicate a consistent mechanism for the multiple reaction involving the five species: H_2, CH_4, H_2O, CO, and CO_2.

METHODS

Apparatus and procedure. The apparatus employed is basically the same as that used in Part II. A mixture of carbon monoxide and hydrogen together with a flow of helium was rapidly recirculated at a rate of 3000 ml/min through a gradientless open-flow reactor over a bed of nickel catalyst (supported on silica, 60 wt% Ni). The feed mixture was injected into the system by a syringe mounted on a movable slide. Outlet gases were analyzed by a Finnigan quadrupole mass spectrometer (Type 1015C) with the electron energy fixed at 50 eV. Raw experimental data corresponding to peak heights of the product species were stored on the disk memory of a Finnigan computer (Series 6000, α-16K). A Prime computer (Model 350) was used to model the data.

Prior to each experiment the catalyst was initially reduced in a flow of hydrogen for a period of 2 h at the reaction temperature. A mixture of carbon monoxide and hydrogen was then introduced into the system with the syringe until steady state was attained, usually in 1 to 2 h. A small proportion of the outgoing gas stream from the reactor was passed through the mass spectrometer and the intensities of the mass peaks were stored for further calculations to determine the concentration of the product species. The peak heights at m/e = 44, 28, 18, 15, and 2 were used to obtain the flow rates of CO_2, CO, H_2O, CH_4, and H_2, respectively. After steady state was reached the feed mixture was typically replaced by a mixture of ^{13}CO and hydrogen while the flow of helium still continued. It took about 50 min until all the unmarked carbon atoms were replaced by their corresponding tagged elements. In this case, m/e = 45, 29, and 17 were used to determine the evolution in time of $^{13}CO_2$, ^{13}CO, and CH_4. The contribution of the marked species was corrected for the contribution from the mass spectrometric background and the natural abundance of ^{13}C. For m/e = 17, the contribution from water was subtracted prior to determination of the concentration of $^{13}CH_4$. The concentrations reported here are in terms of tracer fractions, z^i defined as in Part I, except that in the present report no correction for natural abundance of ^{13}C in the unmarked carbon monoxide was made, so that the initial marking will correspond to 1.11% of ^{13}C in the unmarked feed. The tracer fraction is the fraction of ^{13}C of the total carbon content of a given species.

In addition to runs in which ^{13}CO was marked, some experiments were conducted in which $^{13}CO_2$ was mixed with the inlet CO/H_2 stream. Also supplementary runs were conducted with deuterium transfer to water in the reacting system.

In all cases operation was conducted

close to atmospheric pressures and at 210°C.

As discussed in Part II, a technique described as "washing" was employed in conjunction with the basic superposition technique employed in that study. This technique provides positive quantitative confirmation that the values of chemisorbed carbonaceous species computed by modeling are in reasonable agreement with the same values obtained directly. In a typical experiment using this "washing" technique a mixture of hydrogen, carbon monoxide and helium is fed to the reaction system until steady state methanation is reached. Then instead of performing a tracer experiment, the unreacted species are desorbed by purging with helium and the amounts of such desorbed species are estimated by gas analysis of the effluent. The chemisorbed intermediates, that would require reaction with hydrogen to render them removable, remain on the catalyst. These intermediates are then "titrated" by switching to a feed stream consisting of deuterium and analyzing for the deuterated methanes recovered in the effluent. Thus the total CD_4 obtained corresponds to adsorbed carbon on the catalyst in all forms. At the end of an experiment the temperature is raised to insure that all carbon will be removed. In fact very little additional carbon is obtained in this manner, indicating that little graphitic unreactive carbon is present. Similarly CHD_3 production corresponds to CH adsorbed; CH_2D_2 corresponds to CH_2 adsorbed; CH_3D corresponds to CH_3. The values obtained by modeling, which are comparable, of course correspond to the presence of intermediates on the catalyst in its working state.

In Part II data were presented on the characterization of the nickel catalyst by adsorption of separate gases at room temperature. Hydrogen and carbon monoxide adsorption experiments indicated the presence of complete monolayer coverage corresponding to 14 ml/g of atomic hydrogen sites.

Method of correlation. The system being considered is assumed to consist of a number of compartments, each containing an intermediate or one of the terminal species. Such a system can be described by a set of simultaneous differential equations, each representing the rate of change of fractional marking in these compartments.

As in Parts I and II a nonlinear least squares regression technique was employed to estimate the model parameters. It was assumed that net concentration of intermediates, including both marked and unmarked species, are time invariant since the overall reaction remains at steady state through an experiment. This assumption is consistent with the fact that the kinetic isotopic effects were observed to be negligible in the case of ^{13}C tracing and did not exceed 5–10% in the case of deuterium.

In the case of ^{13}C tracing the fractional marking of the species are taken as the dependent variables as in I. However, the assumption of unidirectional transfer from CO separately to CO_2 and CH_4 enables considerable improvement in the modeling procedure over that employed in Part I. The modeling can be subdivided into three separate steps. In the first CO alone is modeled to obtain CO_l. In the second step transfer between ^{13}CO and $^{13}CH_4$ is modeled and in the third transfer between ^{13}CO and $^{13}CO_2$. This reduces the number of parameters, since all three of these steps were modeled together in Part I. In the present study it is thus possible to consider the existence of two different forms of carbon: reactive (C^a_l) and unreactive (C^*_l). The unreactive form reaches a steady state concentration, so that it does not contribute to catalyst deactivation with time.

As noted in Part II, when deuterium is used as a tracer it is more useful to take the actual concentrations of deuterated species as dependent variables. This is because the carbon-containing species CH_4, CO, and CO_2 each contain only an atom of carbon but the hydrogen-containing species usually contain more than one hydrogen atom.

Thus in the case of transfer between hydrogen and water the species H_2, HD, HOD, and H_2O are present along with H*l*, OH*l*, D*l*, and OD*l*. Information would be lost by using only fractional deuterium marking.

RESULTS

Several sets of experiments were conducted in order to supplement the information presented in Parts I and II. Results are summarized in appropriate tables and compared with data in figures. The equations for modeling and results are considered separately in the following sections.

Tracing of Carbon Monoxide and Methane

A model similar to that in Part I was employed except that two types of carbon species are assumed, as follows:

$$\begin{aligned}
CO + l &\overset{v_1}{\rightleftharpoons} COl \\
COl + l &\overset{v_2}{\rightarrow} C^{a}l + Ol \\
C^{a}l &\overset{v_3}{\rightleftharpoons} C^{*}l \\
C^{a}l + Hl &\overset{v_4}{\rightarrow} CHl + l \\
CHl + Hl &\overset{v_5}{\rightarrow} CHl + l \\
CHl + Hl &\overset{v_6}{\rightarrow} CHl + l \\
CHl + Hl &\overset{v_7}{\rightarrow} CH + 2l
\end{aligned} \qquad (1)$$

The first step is at equilibrium and the step velocities are rapid so they cannot be determined. The second step is unidirectional. The third step, exchange between active and inactive carbon is at equilibrium but need not be rapid since this exchange v_3 is not related to the methane formation rate. The remaining steps are taken as unidirectional and via atomic hydrogen in accordance with modeling data in Part II. The model as shown would require determination of the following seven parameters: C^{COl}, C^{Cal}, C^{C^*l}, C^{CHl}, C^{CH_2l}, C^{CH_3l} and the exchange velocity v_3. Tracing will not enable all these parameters to be determined but useful simplifications can be made based on Part II. Deuterium tracing showed that concentrations of CH_2l and CH_3l were much smaller than that of CH*l* so it was decided to lump these three species as CH_xl since they could not be uniquely identified. The lumped parameter CH_xl may be slightly larger than the sum of CH*l*, CH_2l, and CH_3l concentrations since a sequence of compartments will contribute greater delay than a single compartment with the same total concentration. Deuterium washing showed that the sum of the $C^{a}l + C^{*}l$ species concentrations is comparable to that of CH_xl except at very low H_2/CO ratios. Computer modeling over a spectrum of assumed initial parameter values within limits found by deuterium washing and tracing gave unique solutions always corresponding to low values of $C^{a}l$.

Material balances for the mechanism given by Eq. (1) are as follows, leaving out the balances for C^{COl} which can be determined separately:

$$\begin{aligned}
\frac{dz^{C^{a}l}}{dt} &= \frac{V}{C^{C^{a}l}}\left(z^{COl} - z^{C^{a}l}\right) \\
&\quad - \frac{v_3}{C^{C^{a}l}}\left(z^{C^{a}l} - z^{C^{*}l}\right) \\
\frac{dz^{C^{*}l}}{dt} &= \frac{v_3}{C^{C^{*}l}}\left(z^{C^{a}l} - z^{C^{*}l}\right) \\
\frac{dz^{CH_xl}}{dt} &= \frac{V}{C^{CH_xl}}\left(z^{C^{a}l} - z^{CH_xl}\right) \\
\frac{dz^{CH_4}}{dt} &= \frac{VW}{\beta C^{CH_4}}\left(z^{CH_xl} - z^{CH_4}\right)
\end{aligned} \qquad (2)$$

where:

C^{il} = concentration of chemisorbed species, $i = C^{a}$, C^{*}, CH_x, ml/g (STP)
C^{CH_4} = concentration of gas phase CH_4, volume fraction
t = time following initial change to ^{13}CO, min
V = rate of production of methane, ml/min/g (STP)
W = weight of catalyst, g
β = volume of dead space, ml

z^{CO} and z^{CH_4} are observed as functions of time.

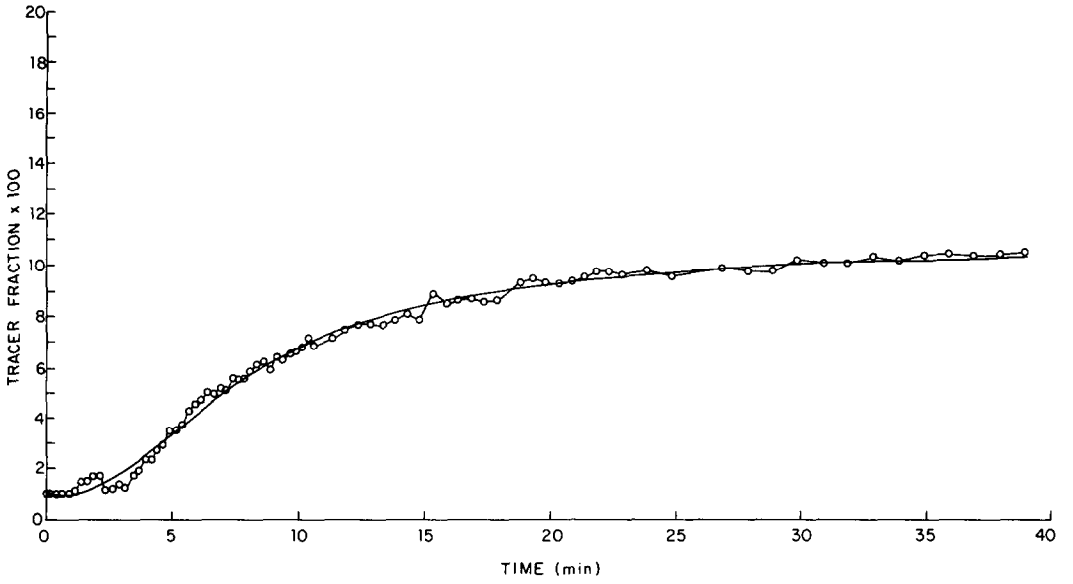

FIG. 1. $^{13}CH_4$ transient Run 091577. Experimental data: (O) CH_4. Calculated (—).

Based originally on deuterium tracing data reported in Part II, it was first decided to reexamine the results reported in Part I. It was noted that for the experiments reported at H_2/CO ratios of 4/1 and 3/1, Figs. 10 and 11 in that paper, the observed values of z^{CH_4} did not rise as rapidly at long contact times as would be indicated by the model. Modeling these data by Eq. (2) resulted in much better agreement with the z^{CH_4} curves as shown in Figs. 1 and 2. Table 1 gives the new values for parameters based on data detailed in Table 8 of the original study (Part I). It is seen that the concentration of

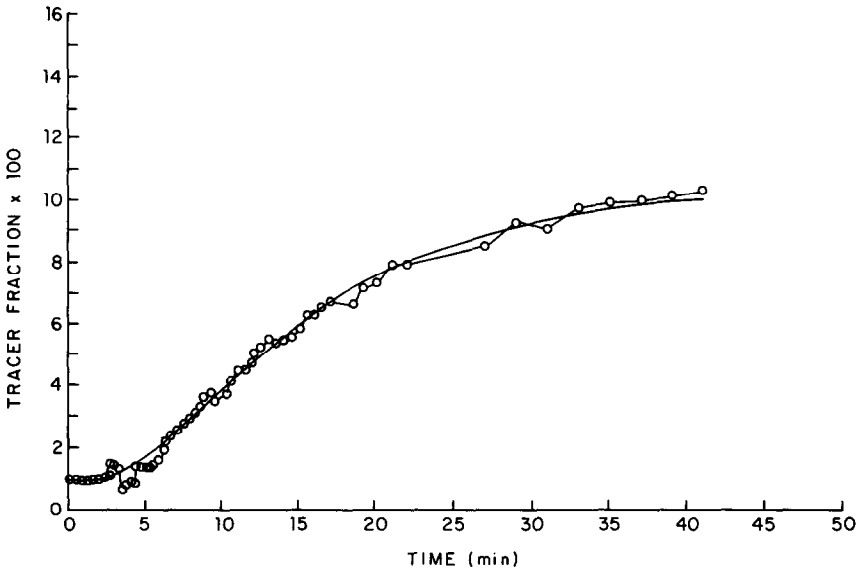

FIG. 2. $^{13}CH_4$ transient-Run 092577. Experimental data; (O) CH_4. Calculated (—).

TABLE 1

CO Step-up—211°C[a]

Calculated surface concentration (ml/g)	Exchange velocity, ml/min/g (NTP)	
	Run No. 091577	Run No. 092577
$C^a l$	0.16 ± 2.74	0.44 ± 4.89
$C^* l$	0.68 ± 0.49	0.61 ± 2.55
$CH_x l$	0.11 ± 1.78	0.20 ± 2.39
υ_3	0.09 ± 0.13	0.09 ± 0.38

[a] For data corresponding to these runs refer to Table 8 of Part I.

[b] Deviations for parameters are computed estimates of standard errors.

inactive carbon is somewhat higher than that of active species though the values of this parameter are not determined with great accuracy.

It was therefore decided to obtain additional ^{13}CO tracing data in the range of lower H_2/CO ratios, using the improved apparatus described in Part II. Results of this study using ^{13}CO step-up experiments are given in Table 2. The four runs for this series are shown in Figs. 3–6. These experiments were conducted at the same temperature (211°C) and atmospheric pressure but with varying H_2/CO ratios. In Table 2 parameters ($C^a l$), ($C^* l$), ($CH_x l$), and (υ_3) were estimated from methane modeling using Eqs. (2). Additional parameters appearing in this table were determined separately

TABLE 2

^{13}CO Step-up—211°C[a]

	Run No.[c]			
	011680	110879	011080	012880
Inlet flow rates (ml/min) NTP				
H_2	4.47	2.13	1.43	0.63
CO	1.18	0.71	1.43	1.24
He	99.23	81.30	83.02	82.25
Inlet fractional marking				
z	19.27	24.50	18.56	19.44
Outlet flow rates (ml/min) NTP				
H_2	2.35	1.14	0.69	0.24
$^{13}CO + CO$	0.31	0.33	1.29	1.26
$^{13}CH_4 + CH_4$	0.80	0.37	0.23	0.13
$^{13}CO_2 + CO_2$	0.006	0.04	0.04	0.06
H_2O	0.88	0.31	0.29	0.15
Calculated surface concentration (ml/g) exchange velocity (ml/min/g) NTP[b]				
$C^{Ca}l$	0.08 ± 0.25	0.20 ± 0.63	0.07 ± 0.44	0.05
$C^{C*}l$	2.17 ± 0.90	2.07 ± 1.15	1.76 ± 0.10	10.53
$C^{CH_x}l$	1.75 ± 1.33	1.14 ± 2.08	2.15 ± 0.05	0.73
υ_3	0.16 ± 0.19	0.16 ± 0.39	0.11 ± 0.00	0.24
$C^{CO}l$	5.31 ± 0.08	5.82 ± 0.03	7.06 ± 0.02	7.28 ± 0.03
$C^{CO_2}l$	0.04 ± 0.00	0.05 ± 0.00	0.04 ± 0.00	0.04 ± 0.00
$C^{CO_2 m}$	0.16 ± 0.00	0.06 ± 0.00	0.11 ± 0.00	0.23 ± 0.07
υ_{10}	0.007 ± 0.000	0.002 ± 0.000	0.004 ± 0.000	0.003 ± 0.001

[a] Weight of catalyst, 2.43 g; pressure, 1 atm; dead space, 118 ml.

[b] Deviations for parameters are computed estimates of standard errors.

[c] An estimate for standard error was not possible for Run 012880.

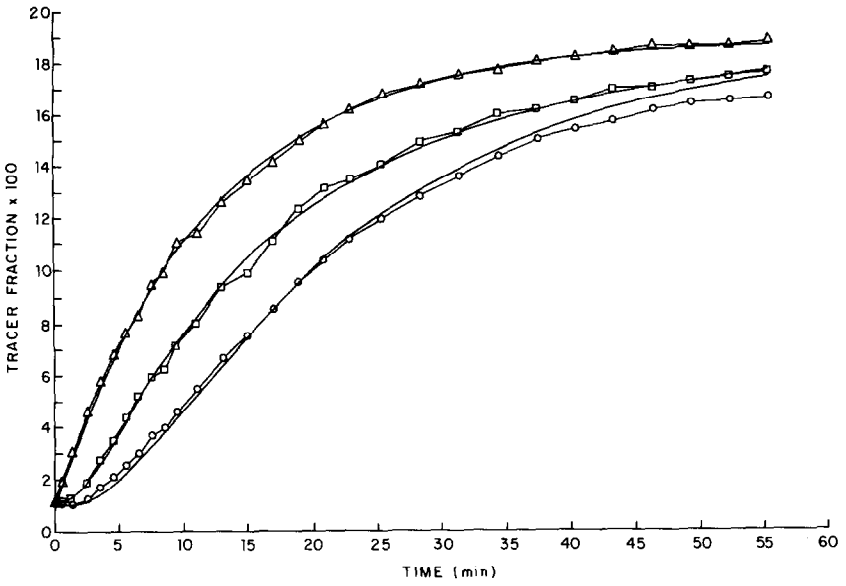

FIG. 3. $^{13}CH_4$, ^{13}CO, and $^{13}CO_2$ transients-Run 011680. Experimental data; (○) CH_4; (△) CO; (□) CO_2. Calculated (—).

from carbon dioxide and carbon monoxide modeling as described later.

Exact comparative interpretation of the data for CH_4 modeling is not possible because the experiments were conducted on catalysts with different levels of activity. However, the concentration of active carbon was always found to be very much less

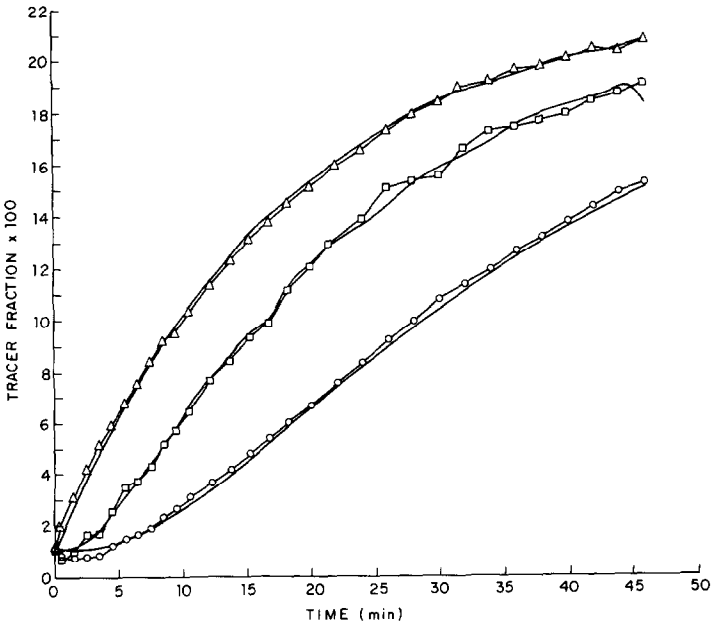

FIG. 4. $^{13}CH_4$, ^{3}CO, and $^{3}CO_2$ transients-Run 110879. Experimental data; (○) CH_4; (△) CO; (□) CO_2. Calculated (—).

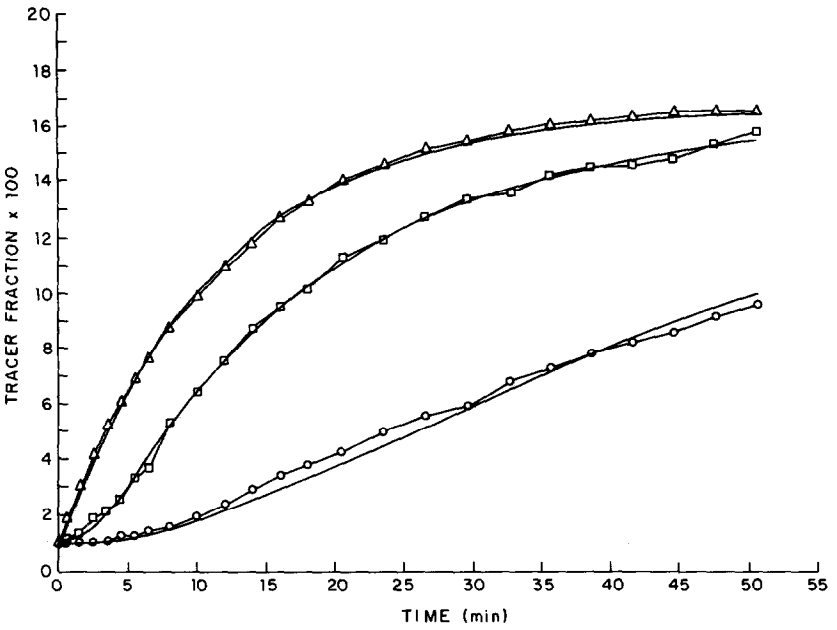

FIG. 5. $^{13}CH_4$, ^{13}CO, and $^{13}CO_2$ transients-Run 011080. Experimental data; (○) CH_4; (△) CO; (□) CO_2. Calculated (—).

than that of the inactive species as also reported in the definitive studies by Goodman *et al.* (*8*). With the exception of Run 011080 the rate of methane production increases with increasing proportions of the CH_xI species. Below a H_2/CO ratio of 0.5, it appears that carbon formation increases very rapidly (Run 012880). Our deuterium tracing study in Part II confirms this conclusion. Gardner and Bartholomew (*9*) reported that for H_2/CO ratios below 0.25 the production of methane is totally inhibited by formation of a large pool of polymeric carbon on a nickel catalyst. While ^{13}CO tracing cannot distinguish between the CH_x intermediates, our deuterium study (Part II)

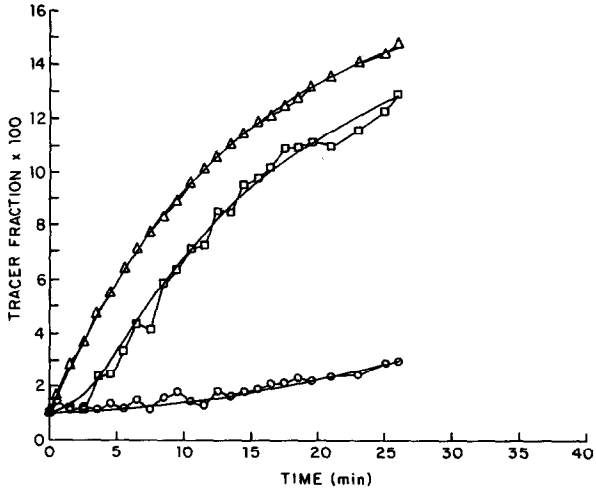

FIG. 6. $^{13}CH_4$, ^{13}CO, and $^{13}CO_2$ transients-Run 012880. Experimental data; (○) CH_4; (△) CO; (□) CO_2. Calculated (—).

showed that the intermediates (CH_2l) and (CH_3l) never exceeded 40% of the concentration of (CHl). Subtracting the possible contributions of (CH_2l) and (CH_3l) from the estimated (CH_xl) parameter, we find that the concentration of (CHl) is still much greater than the concentration of active carbon (C^al).

Tracing Carbon Monoxide Alone

Since it is possible to assume unidirectional transfer of carbon produced by dissociation of carbon monoxide to both carbon dioxide and methane and since adsorption of undissociated carbon monoxide is at equilibrium, a single material balance will serve to enable the concentration of adsorbed undissociated COl to be estimated. Following the nomenclature of Part I we may write

$$(\beta C^{CO} + WC^{COl})\frac{dz^{CO}}{dt} = F_i^{CO}z_i^{CO} - W(V + V')z^{CO} - F_0^{CO}z^{CO} \quad (3)$$

where:

F_i^{CO} and F_0^{CO} = inlet and outlet flow rates of CO, respectively (ml/min)

z_i^{CO} = inlet fractional marking of ^{13}CO

V and V' = velocity of methane and carbon dioxide production, respectively (ml/min/g)

C^{CO} = concentration of carbon monoxide in the dead space, vol. fraction

C^{COl} = surface concentration of adsorbed carbon monoxide (ml/g)

W = weight of catalyst (g)

β = dead space (ml)

In Eq. (3) the only parameter to be determined from the transient of ^{13}CO observed in the effluent is C^{COl}. The solution of Eq. (3) is simple since it involves only one exponential. Subject to initial conditions at $t = 0$, $z^{CO} = 0.0111$, the natural ^{13}C abundance in unmarked CO, it is as follows:

$$z^{CO} = 0.0111e^{-bt} + z_i^{CO}(1 - e^{-bt}) \quad (4)$$

where:

$$b = \frac{W(V + V') + F_0^{CO}}{\beta C^{CO} + WC^{COl}}$$

The output ^{13}CO transient in time is easily fitted to obtain an appropriate value of b for a given experiment and this is solved to obtain C^{COl}.

Estimated concentrations of adsorbed carbon monoxide, C^{COl}, are reported in Table 2 and Figs. 3–6. They show the close agreement of z^{CO} data with the model. Values for C^{COl} do not seem to vary much for the four runs reported. It appears that during methanation the available sites are approximately 50% covered with undissociated chemisorbed CO.

Computer estimates of errors in Table 2 are smaller than those reported for the earlier data, Table 1. These errors show the difficulty in obtaining precise resolution of the parameters with ^{13}CO tracing as compared with results reported for deuterium in Part II. It is likely that the forms of carbon are not clearly characterized into just two types. However, important trends such as the very low concentration of reactive carbon C^al and the invariance of COl surface occupancy can be established with some confidence, since they involve more than a single set of values for an individual experiment.

Tracing Between Carbon Monoxide and Carbon Dioxide

The partial mechanism for production of carbon dioxide during methanation is as follows:

$$\begin{aligned} CO + l &\overset{\upsilon_1}{\rightleftharpoons} COl \\ COl + l &\xrightarrow{\upsilon_2} C^al + Ol \\ COl + Ol &\xrightarrow{\upsilon_8} CO_2l + l \\ CO_2l &\xrightarrow{\upsilon_9} CO_2 + l \\ CO_2 + m &\overset{\upsilon_{10}}{\rightleftharpoons} CO_2m \end{aligned} \quad (5)$$

This model is an elaboration of that reported in Part I. It assumes that adsorbed carbon dioxide CO_2^l can be formed prior to its evolution into the gas phase. The model requires determination of the parameters ($C^{CO_2 m}$), ($C^{CO_2 l}$) and the exchange velocity v_{10}. Material balances are as follows:

$$\frac{dz^{CO_2 l}}{dt} = \frac{V'}{C^{CO_2 l}}(z^{CO l} - z^{CO_2 l})$$

$$\frac{dz^{CO_2 m}}{dt} = \frac{v_{10}}{C^{CO_2 m}}(z^{CO_2} - z^{CO_2 m})$$

$$\frac{dz^{CO_2}}{dt} = \frac{VW}{\beta C^{CO_2}}(z^{CO_2 l} - z^{CO_2}) - \frac{v_{10}W}{\beta C^{CO_2}}(z^{CO_2} - z^{CO_2 m}) \quad (6)$$

where v_{10} = exchange velocity in ml/min/g (STP), V' = rate of CO_2 formation in ml/min/g (STP). At $t = 0$, $z^{CO} = z^{CO_2} = 0.0111$, corresponding to the natural abundance of ^{13}C.

The exchange mechanism used, of course, involves several steps. The parameters $C^{CO_2 l}$, $C^{CO_2 m}$, and v_{10} are given in Table 2 and the corresponding tracer data in Figs. 3–6. Both exchange velocities and surface concentrations are small. Although these parameters appear to be satisfactorily modeled, it is not possible to place as much confidence in them as for the parameters determined by the $^{13}CH_4$ transient. The small proportion of CO_2 production relative to H_2O in methanation over nickel reduces the accuracy of the $^{13}CO_2$ determination. Also, as noted in Part I, independent tracing by $C^{18}O$ is difficult, probably due to ^{18}O exchange with the catalyst support.

TABLE 3

Steady-State ^{13}CO Marking Experiment[a]

	ml/min	
	Inlet rate	Outlet rate
CO	0.62	0.043
H_2O	0.00	0.41
H_2	1.87	0.56
CH_4	0.00	0.51
CO_2	0.31	0.46

Note. Reaction temperature = 211°C. He flow rate = 93.62 ml/min (NTP). Marking of inlet CO_2, fraction of $^{13}CO_2$, $z^{CO_2} = 0.9$ at a time of 47 min after introduction of $^{13}CO_2$. Marking of exit $^{13}CH_4$, fraction of $^{13}CH_4$, $z^{CH_4} = 0.1$. Marking of exit ^{13}CO, fraction of ^{13}CO, $z^{CO} = 0.08$. Estimated value of $V_-^{8,9}$ = 0.005 ml/g catal. (NTP)

[a] Weight of catalyst, 2.43 g; pressure, 1 atm; dead space, 118 ml.

To further corroborate the slow backward transfer of CO_2, experiments were conducted in which $^{13}CO_2$ marking was used in place of ^3CO. The mass balance for the CO_2 compartment corresponding to Eq. (6) would now require a contribution for the velocity v_{-9}, as follows:

$$\frac{dz^{CO_2}}{dt} = \frac{(V' + v_{-9})}{\beta C^{CO_2}/W}(z^{CO} - z^{CO_2}) + \frac{v_{10}}{\beta C^{CO}/W}(z^{CO_2 m} - z^{CO_2}) + \frac{F_i^{CO}}{\beta C^{CO_2}}(Z_i^{CO_2} - z^{CO_2}) \quad (7)$$

For transient tracing the first of Eqs. (6) involving the mass balance for $CO_2 l$ would also require modification. However, it was not possible to employ a high enough concentration of CO_2 to permit transient tracing without altering the kinetics, so steady state tracing was used. A combined velocity was employed to account for both steps 8 and 9 with negative velocities, namely $V_-^{8,9} = v_{-8}v_{-9}/(v_{-8} + v_{+9})$. A derivation for this combined velocity is given by Happel and Csuha (*10*). At the steady state the terms involving closed exchange with the parameters v_{10} and $z^{CO_2 m}$ vanish, so the following single correlating equation applies

$$0 = \frac{(V + V_-^{8,9})}{\beta C^{CO_2}/W}(z^{CO} - z^{CO_2}) + \frac{F_i^{CO_2}}{\beta C^{CO_2}}(Z_i^{CO_2} - z^{CO_2}) \quad (8)$$

z^{CO_2} and z^{CO} are the observed steady state

concentrations and $z_i^{CO_2}$ is the steady state marking level of $^{13}CO_2$. The only unknown is the desired reverse velocity $V_{-}^{8,9}$. The value of this parameter was determined for a $^{13}CO_2$ tracing experiment and is reported in Table 3. $V_{-}^{8,9}$ is equal to 0.005 ml/min/g(NTP), which is about 8% of the rate of CO_2 production.

Tracing Between Hydrogen and Water

The remaining information required to complete the mechanism for the multiple overall reaction corresponds to tracing of the steps whereby hydrogen is converted to water. The tracing of hydrogen to methane has already been presented in Part II. Hydrogen transfers very rapidly to water as well as being at adsorption equilibrium with the atomically adsorbed hydrogen, as discussed in Part II. The following steps may be assumed to occur

$$\begin{aligned} H_2 + 2l &\overset{v_{11}}{\rightleftharpoons} 2\,Hl \\ CO + l &\overset{v_2}{\rightleftharpoons} C^a l + Ol \\ Ol + Hl &\overset{v_{12}}{\rightleftharpoons} OHl + l \\ OHl + Hl &\overset{v_{13}}{\rightleftharpoons} H_2O + 2l \end{aligned} \qquad (9)$$

Since the steps 11, 12, and 13 are close to equilibrium, it is not possible to determine the step velocities or to separate Hl from OHl. If it is assumed that concentrations of the latter, as well as that of water are small, the following relationship can be used to determine the concentration of adsorbed Hl during the methanation reaction.

We write the following balance equation for the total hydrogen holdup:

$$(\beta C_0 + (WC_1)/2) = F_i^{H_2} - (F_0^{H_2} + F_0^{H_2O})z^{H_2} - 2VWz^{H_2} \qquad (11)$$

where:

V = unidirectional rate of methane production, ml/min/g
$F_i^{H_2}$ = inlet flow rate of all hydrogen species (H_xD_{2-x}), ml/min, x = 0–2
$F_0^{H_2}$ = outlet flow rate of all hydrogen species (H_xD_{2-x}), ml/min, x = 0–2
$C_0 = C^{H_2} + C^{HD} + C^{D_2}$, concentration in vapor phase of all hydrogen species, volume fraction
$C_1 = C^{Hl} + C^{Dl}$, concentration of adsorbed protium, ml/g
z^{H_2} = fraction of deuterium in the vapor phase content of hydrogen plus deuterium (protium)
W = weight of catalyst, g
β = dead space, ml

The solution to Eq. (11) is easily obtained as follows:

$$z^{H_2} = 1 - e^{-kt} \qquad (12)$$

where:

$$k = \frac{2VW + F_0^{H_2} + F_0^{H_2O}}{\beta C_0 + WC_{1/2}} \qquad (13)$$

The constant k is derived by obtaining a best fit between the transient of H_2 during deuterium step-up experiments and Eq. (12). The surface coverage of adsorbed hydrogen (H_l) is determined from Eq. (13). It should be noted that Eq. (12) is derived by noting that at steady state the rate of overall production of the hydrogenated species, H_xD_{2-x}, CH_xD_{4-x}, and $H_xD_{2-x}O$ equals the inlet rate of hydrogen or deuterium to the system because the isotopic kinetic effect is small. Although the deuteromethane tracing studies in Part II do not correspond exactly to the present ^{13}C studies, a selection of runs from that paper can be employed to obtain an approximate estimate for atomic hydrogen coverage C_1 for Runs 110879 and 011080 in Table 2. For Run 110879 corresponding to a H_2/CO ratio of 3/1, the estimated C_1 = 4.09 ml/g and for Run 011080 correspond to a H_2/CO ratio of 1/1, c_1 = 2.50. These concentrations were respectively calculated from values for k = 0.165 for Run 021081 and k = 0.31 for Run 083181 in Part II. The other parameters appearing in Eq. (13) are also reported in Tables 1 and 2 of Part II.

DISCUSSION

The studies in this and in the two pre-

vious papers enable a reasonable picture to be drawn for the methanation reaction over nickel catalyst under the conditions of the experiments. Depending on the choice of elementary steps considered plausible a number of mechanisms would be possible for the system.

Happel and Sellers (*11*) presented a procedure that is useful for the separate consideration of possibilities. Application of the method to the methanation system has been discussed by Happel and Sellers (*12*). There are five terminal species involved: H_2, CH_4, H_2O, CO, and CO_2 so the mechanism can be algebraically expressed in terms of two overall simple reactions with appropriate directions provided a sufficient number of elementary steps is postulated. Five such reactions can be obtained by writing equations each with one of the five terminal species omitted but for these studies a convenient choice consists of the following two because of observed rates and thermodynamic restrictions on reaction directions:

$$\begin{aligned} 3H_2 + CO &= CH_4 + H_2O \\ 2H_2 + 2CO &= CH_4 + CO_2 \end{aligned} \qquad (14)$$

Equations (14) are useful for visualizing the reaction system and for the possible development of rate equations, but they do not influence the mechanism as expressed by a combination of elementary steps.

If the dissociation of carbon monoxide is thought to proceed by assistance from hydrogen, oxygenated species like CHO*l* are possible and in that case a large number of mechanisms is possible. However, according to many studies including a recent paper by Yates and Cavanagh (*13*) this is considered unlikely in methanation. It is still possible that interconversion could occur with intermediates similar to those involved in the water gas shift reaction, such as CHOO*l* according to studies of Oki *et al.* (*14*). Transfer via this intermediate alone would not involve the dissociation of CO. If the water gas shift intermediate is involved, it would be presumed that over nickel catalyst an elementary step such as:

$$COl + Ol \rightarrow CO_2l + l \qquad (15)$$

would be very slow so that CO_2l production could be more likely to occur as follows:

$$CHOOl + l \rightarrow Hl + CO_2l \qquad (16)$$

The CHOO*l* could be produced by a reaction step such as:

$$OHl + COl \rightarrow CHOOl + l \qquad (17)$$

One of the models we employed in attempts to correlate the tracer data for CO_2 production employed such a mechanism but it was found to result in too large a delay in $^{13}CO_2$ appearance, if the intermediates are all present in equal proportions. Also the water gas shift reaction is relatively slow under the conditions reported here. The remaining model, which involves neither a CHO*l* or CHOO*l* intermediate fitted the data satisfactorily (model m_8 in Happel and Sellers (*12*)). It is the model corresponding to synthesis of an overall mechanism from the partial mechanisms studied by tracing and may be written as follows:

Reaction Step	Net Rate of Step
$CO + l \overset{v_1}{\rightleftharpoons} COl$	$V + V'$
$COl + l \overset{v_2}{\rightarrow} C^al + Ol$	V
$C^al \overset{v_3}{\rightleftharpoons} C^*l$	—
$C^al + Hl \overset{v_4}{\rightarrow} CHl + l$	V
$CHl + Hl \overset{v_5}{\rightarrow} CH_2l + l$	V
$CH_2l + Hl \overset{v_6}{\rightarrow} CH_3l + l$	V
$CH_3l + Hl \overset{v_7}{\rightarrow} CH_4 + 2l$	V
$COl + Ol \overset{v_8}{\rightarrow} CO_2l + l$	V'
$CO_2l \overset{v_9}{\rightarrow} CO_2 + l$	V'
$CO_2 + m \overset{v_{10}}{\rightleftharpoons} CO_2m$	—
$H_2 + 2l \overset{v_{11}}{\rightleftharpoons} 2Hl$	$3V–V'$
$Ol + Hl \overset{v_{12}}{\rightleftharpoons} OHl + l$	$V - V'$
$OHl + Hl \overset{v_{13}}{\rightleftharpoons} H_2O$	$V–V'$

(18)

In Eqs. (18) the net rate of each mechanistic step is given in terms of the observed rates of methane and CO_2 production according to the best modeled mechanism for the multiple reaction system. Note that there are no steps which seem to require finite reverse reactions that are not large. Steps 1, 3, 10, 11, and 12 are close to equilibrium so only the net rates of these reactions can be determined from the overall rate data. Steps 2, 4, 5, 6, 7, and 8 are close to unidirectional. The rate of formation of CO_2 by step 9 is taken as unidirectional based on ^{13}C modeling. It is much smaller than the rate of water production. The two exchange reactions, steps 3 and 10 are at equilibrium but are slow and do not enter directly into the reaction mechanism.

Values for the surface concentration parameters indicate that the predominant surface species in the mechanism is chemisorbed CO*l*. It will be recalled that complete surface coverage corresponds to about 14 ml/g, the occupancy of undissociated CO alone on the catalyst. During methanation CO*l* seems to be occupying almost half of the total sites, up to 7 ml/g. Hydrogen coverage is substantial, in agreement with studies of simultaneous adsorption of hydrogen and CO on nickel. Only a small proportion of the surface is occupied by active carbon ($C^a l$). The inactive carbon is somewhat larger, but may not occupy active catalyst sites. It can be removed by titration with deuterium as reported in Part II and the coverage thus obtained is in approximate agreement with that obtained by modeling. At the low temperatures used in this study carbon does not convert unidirectionally to graphitic species as shown by Goodman *et al.* (*8*). The remaining important surface species in addition to H*l* and CO*l* is the surface intermediate CH*l*. Estimates of ($CH_x l$) species by ^{13}C tracing are somewhat lower than corresponding values reported in II by deuterium tracing but the methane production rates are also lower, indicating a rough correspondence of (CH*l*) coverage with methanation activity. If the surface occupancy values for Runs 110879 and 011080 are summed up and the values for C^{Hl} obtained as discussed following Eq. (13) are added rough estimates of total surface occupancy of 13.4 and 13.7 ml/g are obtained. These are close to the entire 14 ml/g of available sites obtained by CO or hydrogen adsorption at room temperature. At the lower ratio of H_2/CO = 1/1 the C^{Hl} concentration is lower than at H_2/CO = 3/1. In the run reported in Table 2 at H_2/CO = 1/2 a much higher concentration of inactive carbon was obtained and the methanation rate was much lower.

The rapid exchange of deuterium with water indicates that steps in oxygen removal are fast. Since steps 4–7 in Eqs. (18) are unidirectional and since CH*l* is the predominant surface species, it is likely that the hydrogenation step 5 in Eq. (18) is rate controlling.

Taken together the results of these three studies provide information that is not yet available from the variety of excellent kinetics and surface science studies of this important reaction. The parameters determined by transient tracing should have more intrinsic significance than these obtained by the familiar Langmuir–Hinshelwood–Hougen–Watson technique. Assumptions such as the Langmuir adsorption theory and the law of mass action are not needed for transient tracing. The transient tracing technique should also have applications in studying other similar catalytic reaction systems.

ACKNOWLEDGMENTS

The authors are grateful to the National Science Foundation for support of this study under Grant NSF-ENG-78-04055. Support for F. Yin as a visiting scholar by the People's Republic of China is also appreciated.

REFERENCES

1. Happel, J., Suzuki, I., Kokayeff, P., and Fthenakis, V., *J. Catal.* **65,** 59 (1980).
2. Happel, J., Cheh, H., Y., Otarod, M., Ozawa, S., Severdia, A., J., Yoshida, T., and Fthenakis, V., *J. Catal.* **75,** 314 (1982).

3. Biloen, P., Helle, J. N., Van der Berg, F. G. A., and Sachtler, W. M. H., *J. Catal.* **81,** 450 (1983).
4. Happel, J., Fthenakis, V., Suzuki, I., Yoshida, T., and Ozawa, S., "Proceedings, 7th International Congress on Catalysis, Tokyo," p. 541. Elsevier, Amsterdam, 1981.
5. Biloen, P., Helle, J. N., and Sachtler, W. M. H., *J. Catal.* **58,** 95 (1979).
6. Araki, M., and Ponec, V., *J. Catal.* **44,** 439 (1976).
7. Cant, N. W., and Bell, A. T., *J. Catal.* **73,** 257 (1982).
8. Goodman, D. W., Kelley, R. D., Madey, T. E., and Yates, J. T., Jr., *J. Catal.* **63,** 226 (1980).
9. Gardner, D., C., and Bartholomew, C., H., *Ind. Eng. Chem. Prod. Res. Dev.* **20,** 80 (1981).
10. Happel, J., and Csuha, R. S., *J. Catal.* **20,** 132 (1971).
11. Happel, J., and Sellers, P. H., *Ind. Eng. Chem. Fundam.* **21,** 67 (1982).
12. Happel, J., and Sellers, P. H., "Advances in Catalysis," Vol. 32. Academic Press, New York, 1983; in press.
13. Yates, J. T., and Cavanagh, R. R., *J. Catal.* **74,** 97 (1982).
14. Oki, S., Happel, J., Hnatow, M. A., and Kanoki, Y., "Proceedings, 5th International Congress on Catalysis" 1972.